Ultrawide-Band Noise Radar in the VHF/UHF Band

Isak P. Theron, *Member, IEEE*, Eric K. Walton, *Fellow, IEEE*, Suwinto Gunawan, and Lixin Cai

***Abstract*— A radar that transmits continuous band-limited random noise is considered. The target impulse response is constructed from the cross correlation of the received signal with the transmitted noise signal. The system uses a fixed-length delay line and relies on the target movement through the range gate. Range profiles of different automobiles are measured with this system and used in a target recognition example.**

***Index Terms*— Random noise, UHF radar, ultrawide-band radar, VHF radar.**

I. Introduction

IT is possible to build a radar that transmits continuous band-limited noise. The target-impulse response can be constructed from the cross correlation of the received signal with the transmitted noise signal.

In 1959, Horton proposed a distance-measuring radar-transmitting modulated noise such that the distance was obtained from the correlation function [1]. A number of noise radar systems have been used for target impulse response measurements. In [2], the correlation was obtained from a digital correlator after converting from microwave to video frequencies. A discussion of a fixed delay line system for ISAR imaging is given in [3]. A more complex noise radar is implemented in [4] using a variable delay line with an intermediate mixing frequency to measure both in phase and quadrature phase components.

We chose the fixed-range gate noise radar concept. Such a system can establish an arc or ring at a fixed distance (or small set of distances) from the antennas called the range gate. A moving target traces out its range profile as it passes through this ring and this profile can serve as a feature for radar target classification systems.

The next section discusses the construction and operation of a test noise radar system operating in the foliage penetration band (50–600 MHz).

II. Radar System Description

A. The Radar

The noise radar relies on the fact that the correlation of a band-limited noise signal with a delayed version of itself has a $(\sin x)/x$ behavior as a function of delay time [2]. Consider the system shown schematically in Fig. 1.

A noise source generates a broad-band noise signal which is fed to a 3-dB power splitter. One of these outputs is connected directly to the transmitting antenna; the other output is propagated through a coaxial cable to produce a delayed signal. The delayed signal is multiplied with the signal from the receive antenna using a wide-band mixer. The output of the mixer is connected to a low-pass filter. This results in the cross correlation of the received signal with the delayed version of the transmitted signal.

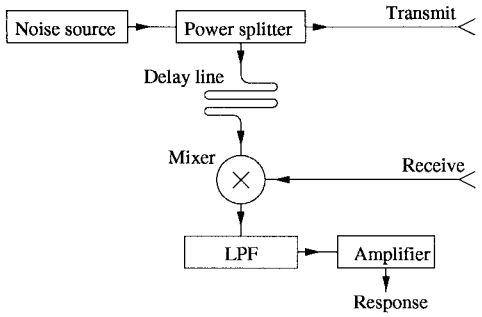

Fig. 1. Schematic representation of the noise radar.

The received signal is the sum of reflections from the target and clutter objects as well as external or environmental noise. White Gaussian noise (of infinite bandwidth) is completely uncorrelated with a delayed version of itself except when the delay is zero. If such a signal is transmitted through an ideal system the output will be zero except if the delay in propagating to and from a point of scattering equals that in the delay line. The output signal is, therefore, proportional to the magnitude of the signal reflected at the distance (called the range gate) for which the propagation time corresponds to the delay time of the delay line. Varying either the length of the delay line or the position of the target thus traces out the impulse response of the target plus clutter [2], [3].

For a noise signal of finite bandwidth the cross correlation has a finite width and the output is the band-limited impulse response. The impulse response is further subjected to dispersion due to the frequency response of the radar system and the radar target. The radar system dispersion effects can be reduced by proper calibration.

The system transmits a continuous noise signal of approximately 20 dBm over the band from 50 to 600 MHz. For a good signal-to-noise ratio (SNR) at the low-pass filter output, the cutoff frequency of the low-pass filter must be as low as possible. As a target moves through the range gate, the impulse response must be traced out. The low-pass filter thus limits the maximum allowable target speed. The cutoff frequency of the low-pass filter is, therefore, a compromise between these two factors. In the present system this frequency is 10 Hz.

B. Antenna System and Setup

This radar uses ultrawide-band signals (50–600 MHz). In addition, it transmits all these frequencies simultaneously and

Manuscript received March 11, 1997; revised March 31, 1999.

The authors are with the ElectroScience Laboratory, Ohio State University, Columbus, OH 43212 USA.

Publisher Item Identifier S 0018-926X(99)05821-4.

calculates the cross correlation of the transmitted and received signals. This requires wide-band antennas with a well-defined phase center over the frequency band. Therefore, a pair of rhombic TEM traveling-wave antennas [5] with excellent wide-band characteristics was used with this system.

Each antenna consists of a pair of rhombic-shaped conducting plates with the spacing between the plates increasing toward the far end. The plates are 2.39 m long with a maximum width of 0.61 m at a distance of 1.17 m from the feed end. At the far end the tips are separated by 1.22 m and are terminated with a 200 Ω resistor to reduce reflections from the tips. The input has an impedance of 100 Ω and requires a balanced feed. This is provided by an ultrawide-band 0/180° hybrid coupler with the output ports connected in series.

The antenna gain increases with frequency and has an average of 10 dB over the 50–600 MHz frequency band. The average effective antenna area is 0.2 m^2 and it decreases with frequency such that the product of these two is approximately constant over this frequency band.

Separate antennas are used for transmit and receive. The two antennas are set up in an open grassy field, separated by 1.83 m, with the centers of the antennas 0.92 m above the ground. Vertical polarization is used. The coupling between the two antennas is approximately -35 dB and increases toward the lower frequencies.

The system uses a 12.8-m range gate. This is obtained with a length of coaxial cable which gives a 85-ns delay.

III. Measurement of the Target Impulse Response

The radar output is a slowly varying function of time representing the impulse response of the moving target as it passes the range gate. As the target moves through the range gate with speed v, the highest frequency in the radar output is $2v/c$ times the highest frequency in the transmitted noise. If the target moves too fast, the 10-Hz low-pass filter may attenuate the more rapid transitions. This effect can be compensated for by deconvolving the low-pass filter impulse response from the radar output. In the present case, the target speed was such that this step was not necessary.

The radar output is a function of target position and calibrating this signal as an impulse response requires knowledge of the target position as a function of measurement time. It is desirable to collect response data at equal intervals of down range distance. In the present experiment, distance was measured with a string tied to the target. The target under test is backed though the range gate starting from the antenna. The string winds off a wheel which opens and closes a magnetic switch as it turns. This produces a series of pulses. Sampling the low-pass filter output at the transitions of these pulses then yields the impulse response of the target at fixed 76-mm (3 in) down-range intervals.

Fig. 2 shows the impulse response of a trihedral measured in this way. The trihedral is 2.37 m long measured along the sides joining at the corner. It is standing on the ground on one of its sides, reflecting essentially as a dihedral. Note that the response does not go to zero as the target moves completely through the range gate toward the antenna. This effect may be due to near-field interactions and clutter blockage.

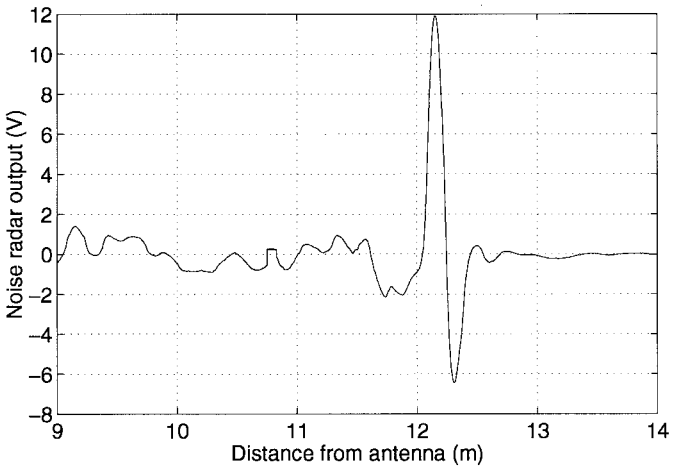

Fig. 2. Uncalibrated impulse response of a 3.35-m trihedral set as a dihedral, measured with the noise radar.

Note that the time axis of the impulse response increases as the target moves toward the antenna. In an operational system where it may not be possible to tie a string to the target, a set of concentric range gates can be used. This will allow the speed and approximate position of the target to be calculated from the raw data.

IV. Frequency Domain Characteristics

As discussed above, the radar measures the target-impulse response as a function of down-range distance or delay time. The Fourier transform of an ultrawide-band impulse response yields both the amplitude and phase of the response as a function of frequency. This section deals with the characteristics of these frequency domain data.

A. Performance in the Presence of Interference

It is important to know how the radar behaves in the presence of interfering receive signals. These signals include externally generated interference and environmental noise as well as thermal noise in the antennas and receiver input stages.

The noise signal at the input to the power divider may be written as a sum of sinusoids with random phase. For a point scatterer measured with an ideal system, the received signal is a copy of this signal with a constant attenuation and time delay. External noise can be written in a similar way with different phase values. The sum of the received signal and the received environmental noise is then multiplied with the delay line signal. For a point scatterer at the range gate, the delay of the received signal will be the same as that of the delayed signal. In this case, it can be shown that for both narrow-band interference and wide-band noise, the output signal to noise ratio is B_s/B_f times the input SNR. Here B_s is the bandwidth of the transmitted signal and B_f is the bandwidth of the low-pass filter. Due to the nature of the correlation process, the best obtainable SNR is $B_s/(2B_f)$—even in the absence of any unwanted signals [6].

The signal processing gain calculated above applies only to the peak response when the target is at the range gate. Measuring the complete impulse response requires moving the target through the range gate. The output signal will decrease away from the range gate while the noise power will not. Thus, a more accurate estimate of the signal processing gain for measuring a complete target response can be obtained by averaging the signal power. Even though the impulse response is infinite in time, most of the information is contained in a region approximately three times the main peak width. The average over this region is approximately 10 dB lower than the peak signal. The signal processing gain is then

$$\text{signal processing gain} = 10\ \log_{10}\frac{B^s}{10B_f} \tag{1}$$

which applies to both single-frequency interference and broadband noise signals.

For the 18 in sphere discussed in the next section, the received signal power is of the order of -50 dBm. Since the transmitted signal is wide-band noise, the direct antenna to antenna coupling will be essentially uncorrelated with the signal received from a target at the range gate. In this application, it will therefore behave in a similar manner to environmental interference. The total interfering power is then approximately -10 dBm. This includes narrow-band interference signals of -20 dBm. Therefore, we have a preprocessing SNR of -40 dB. The signal processing gain given by (1) is 67 dB such that the theoretical postprocessing SNR is 27 dB.

The SNR of the measured signal was also estimated experimentally by comparing the average measured signal power to the average measured noise power. The signal power was averaged over a down-range distance of 1.6 m in accordance with the definition used above and the noise power was averaged on a measurement with no target at the range gate. The resulting experimental SNR was 26 dB. This confirms the theoretically predicted signal processing gain and gives an indication of how the radar behaves in the presence of interference.

B. System Calibration

The Fourier transform of the measured impulse response yields the spectral response of the target. In the present system a 1.8-m-wide gate was applied to the down-range data to isolate the target and zero padding was used to smooth the frequency response. As clutter reflections contribute only a dc component, background subtraction is accomplished by removing the dc offset. For the rest of this section, we will refer to this spectral response when we use the term "measured spectrum" in connection with the noise radar.

This response is, however, subject to frequency dispersion due to the transfer functions of the antennas, transmission lines, the delay line, and the spectral distribution of the noise signal. This unwanted effect may be removed by conventional calibration

$$\tilde{S}_c = \tilde{S}_m \frac{\tilde{S}_{rk}}{\tilde{S}_{rm}} \tag{2}$$

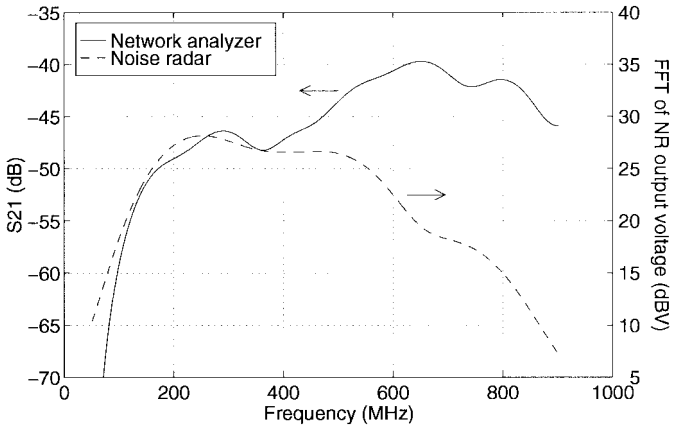

Fig. 3. The spectral response for the trihedral at 12.5 m from the antennas. The network analyzer measurement includes both the target and antenna transfer functions. The noise-radar measurement, obtained from the Fourier transform of the impulse response, also includes the transfer function of the noise radar system. The difference between the two curves gives an indication of the frequency behavior of the noise-radar system.

where $\tilde{S}_c$ is the calibrated response, $\tilde{S}_m$ is the measured response of the target under test, $\tilde{S}_{rk}$ is the known response of a calibration target, and $\tilde{S}_{rm}$ is the measured response of the calibration target.

Calibration requires a calibration target with a known response—bistatic in this case. The targets were in the near field of the antennas as well as over an imperfect ground plane. It was not possible to calculate the theoretical response. The radar performance was, therefore, evaluated by comparing it to a coherent step frequency radar realized with a network analyzer.

The network analyzer measurements were conducted with a 12-ns time-domain gate around the scattering center of the targets. This gate is the same size as the down-range gate used with the noise-radar data. For the network-analyzer measurement, background subtraction was done.

Two targets were measured with both systems. The first is the trihedral discussed previously. Fig. 3 gives the measured spectra for the trihedral using the two systems. The network analyzer response is the measured $\tilde{S}_{21}$, including the effect of the target, the antennas, and the expansion of the spherical wavefronts. The noise-radar measurement is the measured spectrum as discussed at the beginning of this section and includes the same effects as well as the radar transfer function. Note that the scale of this curve is arbitrary as it is not referenced with respect to the transmitted power. The difference between these graphs gives an indication of the noise-radar response as a function of frequency.

The second target was a 457-mm (18-in)-diameter conducting sphere on a plastic sled. For both systems, the measured spectra for the sphere was normalized to that of the trihedral by

$$\tilde{S}_N(f_k) = \frac{\tilde{S}_s(f_k)}{\tilde{S}_t(f_k)} \tag{3}$$

where $\tilde{S}_N(f_k)$ is the normalized response at frequency f_k, and $\tilde{S}_s$ and $\tilde{S}_t$ are the measured spectra for the sphere and dihedral, respectively. Figs. 4 and 5 show the amplitude and phase of the normalized sphere spectrum.

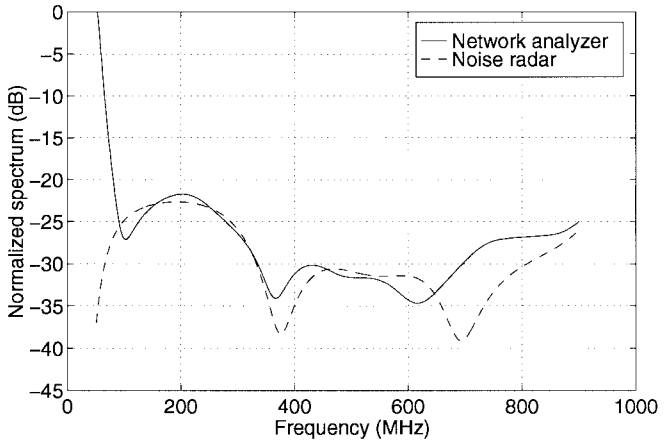

Fig. 4. Amplitude of the spectral response for the sphere normalized to the response of the trihedral.

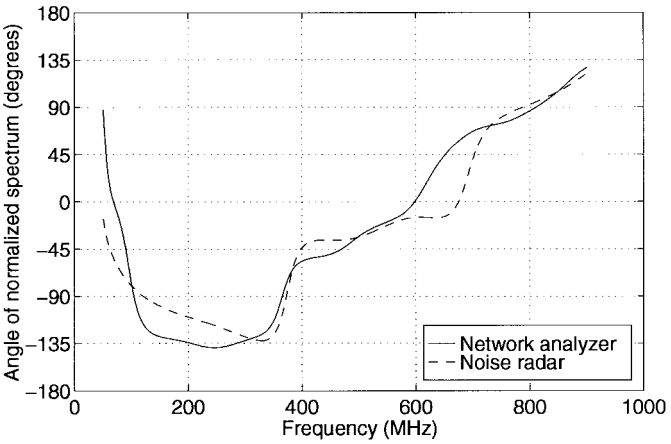

Fig. 5. Phase of the spectral response for the sphere normalized to the response of the trihedral.

The amplitudes compare within a few decibels except at the low-frequency end. Here the network analyzer measurement is highly suspect as the sphere should not reflect almost the same power as the much larger trihedral. This effect is probably due to the time-domain gating and the strong coupling between the antennas at the low frequencies. The agreement between the phase responses is better than 20°, again, except in the low-frequency region. This shows that both amplitude and phase information can be obtained with the noise-radar system as configured here.

V. Automobile Testing

A. Range Profiles

The profiles of a number of different automobiles were measured with the noise-radar system. Two examples are given in Figs. 6 and 7. For comparison, a correctly scaled picture of each vehicle is placed above the graph. The profiles reveal certain reflecting areas such as the front, the windshield, the roof support pillars, and possibly the rear of the vehicle. At the radar frequencies used here, the wavelength varies from 0.5 to 6 m. Much of the scattering is, therefore, likely to be from resonating structures rather than from point-scattering objects.

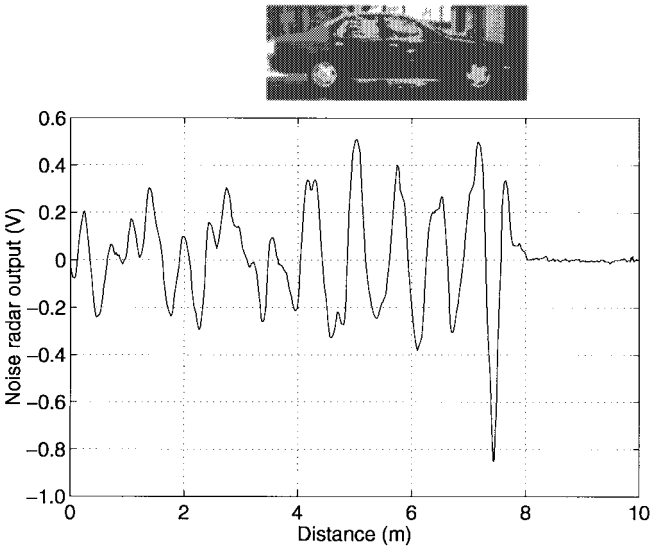

Fig. 6. Response of a four-door 1995 Nissan Altima sedan. The bumper-to-bumper length of the vehicle is 4.47 m.

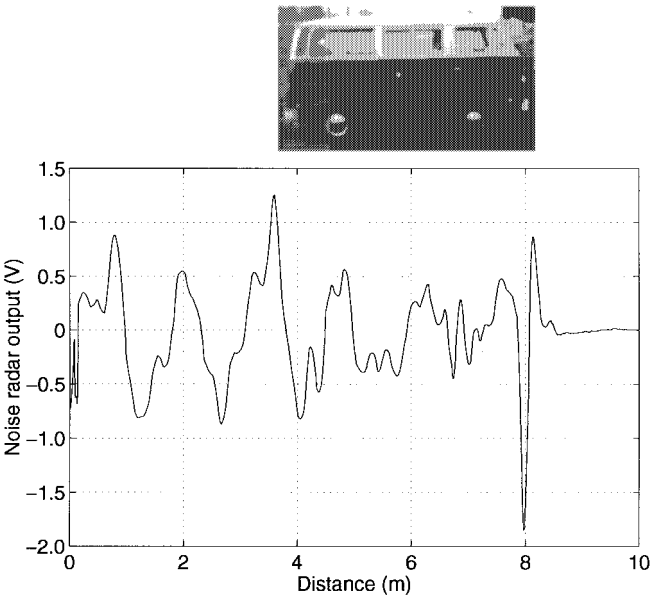

Fig. 7. Response of a 1970 Volkswagen bus. The bumper-to-bumper length of the vehicle is 4.28 m.

In all cases, there is also a significant peak past the back of the vehicle. This may be due to multiple reflections inside the vehicle.

The profiles of the different vehicles indeed differ significantly such that it may be possible to distinguish between these vehicles on the basis of the profiles alone. The differences between different vehicles are certainly significantly larger than for repeated measurements on the same vehicle.

B. Classification Example

A target classification test was done using the cross correlations between our data base of range profiles and a set of "unknown" targets. The unknown targets were generated from the set of measurements by adding zero mean Gaussian

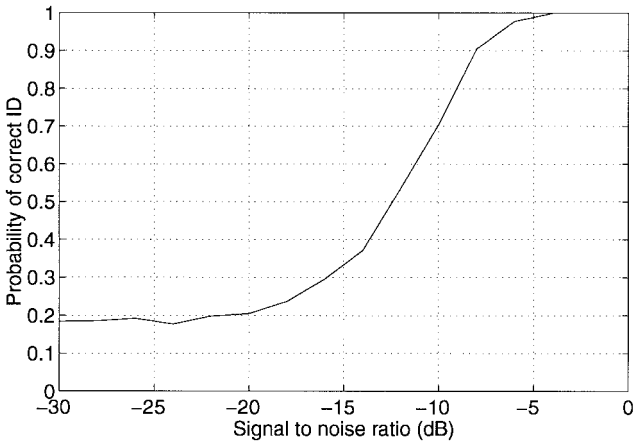

Fig. 8. Probability of correct identification as a function of SNR.

perturbations to the original database. The original database was normalized such that the mean square is the same for all the targets. This removes absolute amplitude as a target classification feature. Each unknown target is then cross correlated with each of these references. The unknown target is "identified" by selecting the reference resulting in the largest peak cross correlation. This was repeated 400 times for each perturbation level for each target. Fig. 8 shows the probability of correct detection as a function of the postdetection SNR's used in the perturbations. Note that it is possible to identify a vehicle with 90% probability of correctness when the perturbations are 8 dB larger than the signal.

VI. Conclusion

We have designed, built, and used an ultrawide-band noise radar that operates in the foliage penetration frequency band (50–600 MHz). We have shown that it is possible to measure the impulse response of a moving target using only a single fixed-range gate. The normalized amplitude and phase as a function of frequency were shown to be similar to those obtained using a coherent step-frequency radar (network analyzer). The noise-radar measured impulse responses of a set of automobiles were shown to be effective as features in a radar classification example.

References

[1] B. M. Horton, "Noise-modulated distance measuring systems," *Proc. IRE*, vol. 47, no. 5, pp. 821–828, May 1959.
[2] G. R. Cooper and C. D. McGillem, "Random signal radar," School Elect. Eng., Purdue Univ., Lafayette, IN, Final Rep. TR-EE67-11, June 1967.
[3] E. K. Walton, V. Fillimon, and S. Gunawan, "ISAR imaging using UWB noise radar," in *Proc. Antenna Meas. Tech. Assoc. (AMTA) Symp.*, Seattle, WA, Sept. 30–Oct. 3, 1996, pp. 167–171.
[4] R. M. Narayanan, Y. Xu, P. D. Hoffmeyer, and J. O. Curtis, "Design and performance of a polarimetric random noise radar for detection of shallow buried targets," in *Proc. SPIE Meet. Detection Technol. Mines Minelike Targets*, Orlando, FL, Apr. 1995, vol. 2496, pp. 20–30.
[5] J. S. Gwynne and J. D. Young, "Time domain characterization of UWB antennas," in *Proc. Antenna Meas. Tech. Assoc. (AMTA) Symp.*, Columbus, OH, Oct. 1992, pp. 1–3, 1–8.
[6] I. P. Theron, E. K. Walton, S. Gunawan, and L. Cai, "Signal to noise ratio calculations and measurements for the OSU noise radar," ElectroSci. Lab., Ohio State Univ., Columbus, OH, Rep. 732168-1, Nov. 1996.

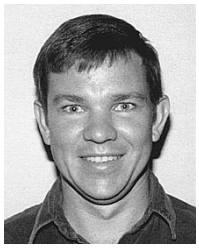

Isak P. Theron (S'89–M'96) was born on August 31, 1967, in Upington, South Africa. He received the M.S. and Ph.D. degrees from the University of Stellenbosch, South Africa, in 1991 and 1995, respectively.

He was appointed as a Postdoctoral Fellow at the University of Stellenbosch, South Africa, in 1996. He served as a Visiting Scholar at the ElectroScience Laboratory, Electrical Engineering Department, The Ohio State University, Columbus, from July 1996 to June 1997. Currently, he is a Postdoctoral Fellow at the University of Stellenbosch and a Research Engineer with EM Software and Systems, Stellenbosch. His research interests include electromagnetic numerical techniques and material properties.

Dr. Theron is a member of ACES.

Eric K. Walton (S'64–M'70–SM'93–F'93) received the B.E.E. degree from the University of Delaware, Newark, in 1966, and the M.S. and Ph.D. degrees from the University of Illinois at Urbana-Champaign, in 1968 and 1971, respectively.

He has been with the ElectroScience Laboratory, Electrical Engineering Department, The Ohio State University, Columbus, since 1978, where he is now a Senior Research Scientist and Adjunct Professor. Over the past 20 years, he has been involved in the study of radio and radar signal analysis, radar target phenomenological studies, and the development of new radar scattering instrumentation. Related research topics include humanitarian land mine mitigation, radar target identification, model-based inverse synthetic aperture radar imaging, higher order spectral analysis (bispectral analysis), and time frequency (multiresolution) analysis of radar scattering.

Dr. Walton served as President of the Antenna Measurement Techniques Association in 1989, having served as Vice Chairman in 1987 and 1988. He has served as secretary (1979), Vice Chairman (1980), and Chairman (1981) of the Columbus, OH, section of the IEEE Antennas and Propagation Society. He is a member of Tau Beta Pi, Eta Kappa Nu, and Sigma Xi.

Suwinto Gunawan was born in Medan, Indonesia, in June 1973. He received the B.S. degree in electrical enginering from Michigan Technological University, Houghton, in 1995, and the M.S. degree from The Ohio State University, Columbus, in 1998.

He was a Graduate Student Associate at the Electrical Engineering Department, ElectroScience Laboratory, The Ohio State University, from 1996 to 1998. He is now with the Motorola Cellular Sector, Libertyville, IL, where he is engaged in the design and development of various wireless communication products. His research interests include random signal radar, radar imaging, signal processing, and wireless communication.

Dr. Gunawan is a member of Tau Beta Pi.

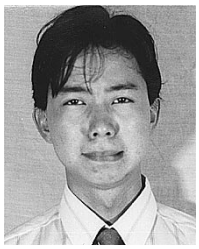

Lixin Cai received the B.S. degree in electrical engineering and applied physics from Case Western Reserve University, Cleveland, OH, and the M.S. degree in electrical engineering from The Ohio State University, Columbus. He is currently working toward the Ph.D. degree in electrical engineering at the ElectroScience Laboratory, The Ohio State University.

He has been with Electroscience Laboratory, The Ohio State University, since 1993. His areas of interest include analytical and computational electrodynamics, transient electromagnetics, forward/inverse scattering, synthetic aperture radar, conformal antennas, electro-acoustics, and optics.